



Gamma-ray computed tomography to characterize soil surface sealing

Luiz F. Pires^{a,*}, Jose R. de Macedo^b, Manoel D. de Souza^c, Osny O.S. Bacchi^a, Klaus Reichardt^a

^aCenter for Nuclear Energy in Agriculture, USP. C.P. 96, C.E.P. 13.400-970 Piracicaba, SP, Brazil

^bEmbrapa Soils, Rua Jardim Botânico, 1024, C.E.P. 22.260-000 Rio de Janeiro, RJ, Brazil

^cEmbrapa Environment, C.P. 69, C.E.P. 13.820-000 Jaguariúna, SP, Brazil

Received 19 November 2001; accepted 14 February 2002

Abstract

The application of sewage sludge as a fertilizer on soils may cause compacted surface layers (surface sealing), which can promote changes on soil physical properties. The objective of this work was to study the use of gamma-ray computed tomography, as a diagnostic tool for the evaluation of this sealing process through the measurement of soil bulk density distribution of the soil surface layer of samples subjected to sewage sludge application. Tomographic images were taken with a first generation tomograph with a resolution of 1 mm. The image analysis opened the possibility to obtain soil bulk density profiles and average soil bulk densities of the surface layer and to detect the presence of soil surface sealing. The sealing crust thickness was estimated to be in the range of 2–4 mm. © 2002 Elsevier Science Ltd. All rights reserved.

Keywords: Computed tomography; Soil compaction; Gamma-ray transmission

1. Introduction

In the last two decades, many studies have been carried out using the gamma-ray computed tomography (CT) technique in several areas of knowledge other than medicine. The gamma-ray CT can be applied for wood density analysis, fatigue tests of asphalt mixtures, and to provide information on the chemical composition of materials (Naime et al., 2000; Macedo et al., 2000; Braz et al., 1999; Robert-Coutant et al., 1999). In soil science, the use of CT scanning was introduced to measure soil density, soil water content, and soil water movement (Crestana et al., 1985; Hainsworth and Aylmore, 1983; Petrovic et al., 1982). Recently, the neutron CT has been utilized to study soil compaction (Lopes et al., 1999) and

portable gamma-ray CT was used in the field for water infiltration studies (Naime, 2001).

Soil surface sealing is an important phenomenon that may occur in the soil surface as a result of clay migration/orientation process and pore plugging. The impact of raindrops promotes the disintegration of soil aggregates and the dispersion of the clay particles in the soil suspension. The finest particles in suspension migrate into soil pores along with water, plugging these pores. During the drying process, deposition, migration, and orientation lead to the formation of a fine hard surface layer (Baver et al., 1973). This layer reduces the time for surface flooding, increasing run-off volume, favoring laminar and furrow erosions (Pagliai and Vignozzi, 1998; Pla, 1985).

The application of sewage sludge as a fertilizer causes additional surface sealing, affecting soil physical properties (Macedo et al., 2001). Scientific results indicate that the effects of the application of sewage sludge are mainly

*Corresponding author. + 55-19-3429-4600x4712; fax: + 55-19-3429-4610.

E-mail address: lfpres@cena.usp.br (L.F. Pires).

caused by the large amount of organic matter present in this residue (Bernardes, 1982). After the incorporation of the sludge into the soil, some of its properties may be altered such as: soil bulk density and porosity (Marciano, 1999; Moraes, 1990), soil water retention capacity (Moraes, 1990), aggregate stability (Logan et al., 1996; Logan and Harrison, 1995; Epstein, 1975), surface compaction or sealing, resistance to penetration, water infiltration, soil hydraulic conductivity, and also the thermal capacity of the soil (Marciano, 1999).

The objective of this work was to evaluate the gamma-ray CT technique as a tool to (i) identify differences in soil density due to the sewage sludge application (ii) determine the sealing crust density and thickness in the compacted layers.

2. Theory

The gamma-ray CT is based on the electromagnetic interaction process that occurs when this radiation crosses different materials (Wang et al., 1975). When a gamma-ray beam passes an homogeneous material of thickness x (cm), the photons are transmitted following the Beer–Lambert law:

$$I = I_0 \exp(-\mu x) = I_0 \exp(-\mu^* \rho x), \quad (1)$$

where I_0 and I are, respectively, the rates of the incident and the emerging photon beams, μ (cm^{-1}) is the linear attenuation coefficient that measures the photon absorption or scatter probability per unit length while interacting within the sample, ($\mu^* = \mu/\rho$) ($\text{cm}^2 \text{g}^{-1}$) is the mass attenuation coefficient, and ρ (g cm^{-3}) is the density of the crossed material.

The application of the gamma transmission technique to heterogeneous and porous materials as soil permits only to obtain the average density values along the radiation path of thickness x (cm) within the sample. The method does not allow the investigation of density variations along the path of length x (cm). However, with the use of CT it is possible to obtain images of transversal sections of a sample, with millimetric resolution (1 mm) (Macedo et al., 1998; Crestana and Vaz, 1998).

With the first generation tomographs, the measurement of photons transmitted along the sample is made in various directions in the same plane in different angles (called angular steps), until a scan of 180° is completed. In each direction, measurements are taken in different parallel positions separated by a constant distance called a linear step. The dataset is stored and processed in a computer to obtain a reconstructed tomographic image.

The gamma beam attenuation in each direction allows the generation of a number called tomographic unit

(TU)¹ with dimension 1/m, that is related to the attenuation coefficient of the soil in each crossing point. Due to the fact that soil samples are generally 2-component heterogeneous mixtures, and that the attenuation coefficients are different for all of its extension, there is a relation between TU and the μ of the sample given by:

$$\text{TU}(E_\gamma) = \alpha \mu(E_\gamma) = \alpha [\mu_s^*(E_\gamma) \rho_s + \mu_w^*(E_\gamma) \theta], \quad (2)$$

where E_γ (keV) is the gamma photon energy, α is the correlation between the linear attenuation coefficient and the TU, μ_s^* and μ_w^* ($\text{cm}^2 \text{g}^{-1}$) are the mass attenuation coefficients of soil and water, respectively, and θ ($\text{cm}^3 \text{cm}^{-3}$) is the volumetric water content.

The differences in TU associated with each point of the soil matrix can be associated with intensity differences within the reconstructed image. White regions correspond to points with higher values of μ and dark regions to lower values. Variation in gray levels correspond to differences in the attenuation coefficients and consequently, to differences in soil density at each point. It is therefore possible to obtain images that present the density distribution of the sample within the tomographic section (Eq. (3)). In the case of a moist soil sample, this density distribution includes the water content distribution. On the other hand, if the soil sample is dry or its water content is uniformly distributed, the TU distribution reflects only the soil bulk density distribution.

$$\rho_s = \frac{\text{TU}}{\alpha(\mu_s^* + \mu_w^* \theta)}. \quad (3)$$

3. Materials and methods

Soil samples for gamma-ray CT analysis come from an experimental field consisting of 36 plots (6 treatments [4 sludge rates + 2 controls (absolute control² and control with NPK³)], using split-plot blocks with three replicates). The rates of sludge were calculated on the basis of dry weight of sludge, that correspond to: 10, 20, 40, and 80 kg m^{-2} and here identified as 1N, 2N, 4N, and 8N, respectively.

Soil samples were collected in cylinders of 3 and 5 cm high at soil surface. A total of 108 undisturbed samples were taken from these treatments. CT and gamma-ray

¹ TU takes the air as the media with the minimum possible μ value. It is linearly related to Hounsfield Unit (HU) that takes the water as a reference media for which $\text{HU} = 0$.

² The term absolute control refers to the control plots that did not receive neither sewage sludge nor inorganic fertilizer.

³ Control with refers to the control plots that did not receive sewage sludge but received N = nitrogen, P = phosphorus and K = potassium.

transmission analysis were performed on 12 and 108 samples, respectively.

A first generation tomograph with fixed source-detector arrangement and translation/rotational movements of sample was utilized to obtain the images. The radioactive source used was ^{137}Cs that emits mono-energetic photons, with an activity of 7.4 GBq, and the detector was a 3 in \times 3 in NaI(Tl) scintillation crystal coupled to a photomultiplier tube. Circular lead collimators with diameter of 1 mm were utilized for both source and detector. Data acquisition and translation/rotational movements were controlled by a PC (Fig. 1).

The calibration of the tomograph was obtained through the correlation between linear attenuation coefficients (μ) of different materials using the gamma-ray transmission method, and the respective tomographic units (TU) (Naime, 2001; Cássaro, 1994). The tomographic images of soil samples were taken for vertical planes crossing the center of the sample. TU values of the samples were converted to soil density profiles (ρ_s) using Eq. (3).

The gamma-ray transmission method was used to investigate the variation in average soil density at three

different depths (3, 5, and 12 mm) from soil surface. Samples were always positioned in such a way to allow the gamma beam to cross the central line of the sample. For the transmission method, the soil density was calculated from Eq. (1), considering their water contents (θ):

$$\rho = \frac{-1}{x\mu_s^*} \left[\ln \left(\frac{I_0}{I} \right) + x\mu_w^*\theta \right], \quad (4)$$

where I_0 is the initial photon intensity, whereas I is the intensity after transmission through soil of thickness x (cm).

4. Results

TU and respective attenuation coefficients are shown in Table 1 and Figs. 2 and 3. The obtained values for linear and mass attenuation coefficients for the materials used for calibration, as well as the values of the mass attenuation coefficient of the soil ($\mu_s^* = 0.0836 \pm 0.0025 \text{ cm}^2 \text{ g}^{-1}$) and water ($\mu_w^* = 0.0850 \pm 0.0005 \text{ cm}^2 \text{ g}^{-1}$) are in accordance with those found in the literature for 661.6 keV photons from the decay of ^{137}Cs (Fante Júnior et al., 2000; Ferraz and Mansell, 1979).

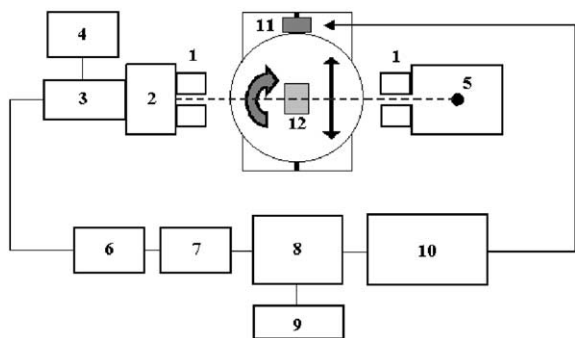


Fig. 1. Schematic diagram of the first generation tomograph (without scale). (1) Lead collimators; (2) NaI(Tl) detector; (3) photomultiplier tube; (4) high-voltage unit; (5) ^{137}Cs source; (6) amplifier; (7) mono-canal analyzer; (8) counter; (9) timer; (10) microcomputer; (11) stepping motor, and (12) soil sample.

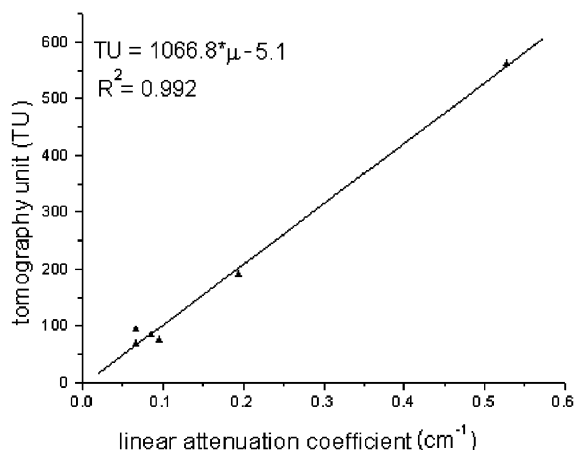


Fig. 2. CT calibration for ^{137}Cs gamma photons.

Table 1

Average values of linear and mass attenuation coefficients and tomographic units for samples utilized to calibrate the gamma-ray tomograph

Sample	μ (cm^{-1})	μ^* ($\text{cm}^2 \text{ g}^{-1}$)	TU
Alcohol	0.06575 ± 0.00020	0.08362 ± 0.00025	67.4 ± 3.7
Nylon	0.09550 ± 0.00025	0.09775 ± 0.00026	75.1 ± 2.8
Water	0.08234 ± 0.00054	0.08234 ± 0.00054	83.3 ± 2.8
Acrylic	0.06662 ± 0.00120	0.05610 ± 0.00101	93.4 ± 3.0
Aluminum	0.19387 ± 0.00099	0.07075 ± 0.00036	190.9 ± 4.4
Brass	0.52732 ± 0.00970	0.06153 ± 0.00113	561.7 ± 7.8

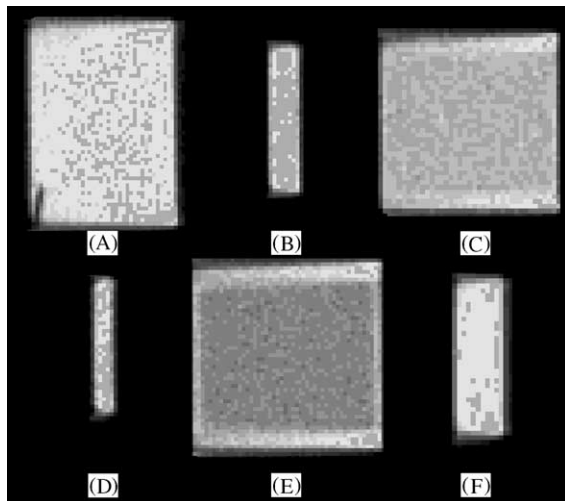


Fig. 3. Tomographic images of samples utilized for the tomograph calibration: (A) aluminum; (B) acrylic; (C) water; (D) nylon; (E) alcohol; and (F) brass.

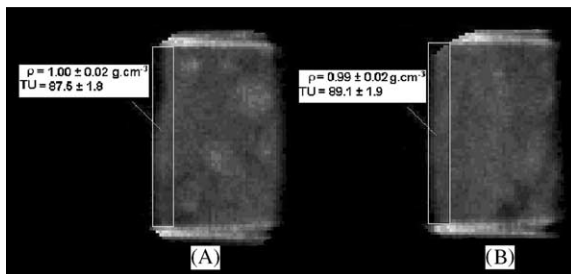


Fig. 4. Tomographic images presenting TU and $\bar{\rho}$ average values for the possibly sealed surface region (cylinder C1): (A) absolute control sample and (B) NPK control sample.

Regarding the analysis of the soil density distribution in the compacted region, it was possible to obtain by CT the average density values of thin layers of the order of 1 mm (Figs. 4–6) and 1.25 mm (Figs. 7–9). Therefore, a more detailed study of the distribution of ρ_s in the sample was possible. Table 2 shows the average densities obtained in possibly sealed regions (ρ_{crust}) and the average soil sample densities (ρ_s), obtained from tomographic images.

Analyzing Table 2 it can be seen that the cylinders C1 and C2 present average densities of the possibly sealed layer (ρ_{crust}) significantly higher in relation to the whole sample bulk density (ρ_s), except for the absolute and NPK control treatments, which did not receive sewage sludge application, and for which the ρ_{crust} and ρ_s values were similar. The tomographic images of Figs. 4 and 7 show values of the average density ($\bar{\rho}$) and TU for the absolute and NPK control treatments evaluated at the possibly sealed region. The values of the average densities for these samples, for the possibly sealed

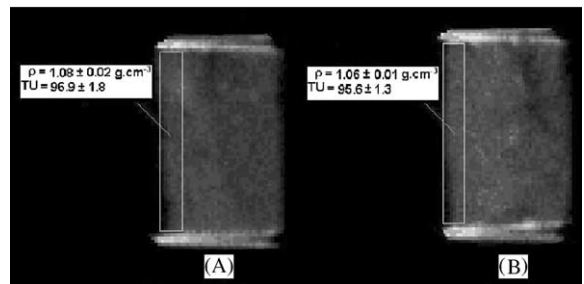


Fig. 5. Tomographic images presenting TU and $\bar{\rho}$ average values for the possibly sealed surface region (cylinder C1): (A) 1N sample and (B) 2N sample.

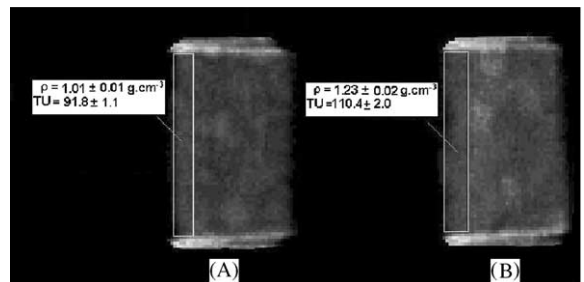


Fig. 6. Tomographic images presenting TU and $\bar{\rho}$ average values for the possibly sealed surface region (cylinder C1): (A) 4N sample and (B) 8N sample.

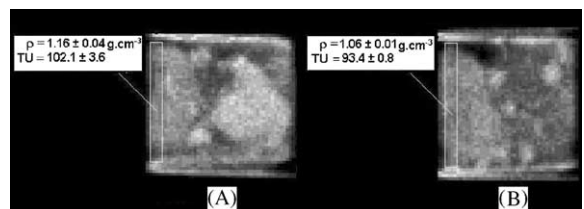


Fig. 7. Tomographic images presenting TU and $\bar{\rho}$ average values for the possibly sealed surface region (cylinder C2): (A) absolute control sample and (B) NPK control sample.

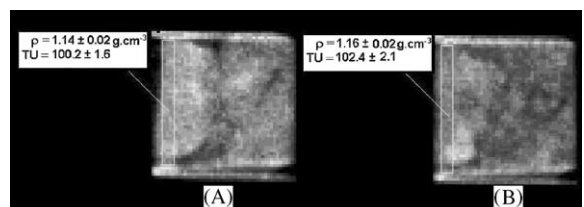


Fig. 8. Tomographic images presenting TU and $\bar{\rho}$ average values for the possibly sealed surface region (cylinder C2): (A) 1N sample and (B) 2N sample.

region, when compared with the whole soil sample average densities (Table 2—columns 4 and 5), indicate the absence of sealing in these treatments.

Figs. 5, 6, 8 and 9 represent samples that received sewage sludge as a fertilizer in the rates 1N, 2N, 4N, and

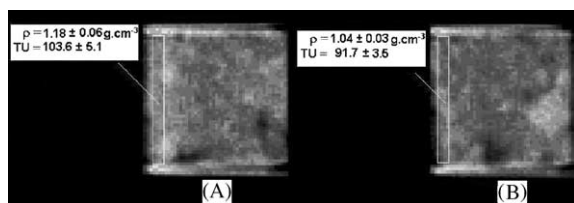


Fig. 9. Tomographic images presenting TU and $\bar{\rho}$ average values for the possibly sealed surface region (cylinder C2): (A) 4N sample and (B) 8N sample.

Table 2

Average soil density values of layers presenting sealing (ρ_{crust}) and soil bulk density (ρ_s) for two cylinders (C1 and C2) of soil samples having received different treatments (Tabs and NPK are controls, 1N, 2N, 4N, and 8N, increasing rates of sewage sludge)

Treatment	ρ_{crust} (g cm^{-3})		ρ_s (g cm^{-3})	
	C1	C2	C1	C2
Tabs	1.00 ± 0.02	1.16 ± 0.04	1.01 ± 0.04	1.14 ± 0.10
NPK	0.99 ± 0.02	1.06 ± 0.01	1.01 ± 0.07	1.01 ± 0.06
1N	1.08 ± 0.02	1.14 ± 0.02	0.96 ± 0.07	1.03 ± 0.10
2N	1.06 ± 0.01	1.16 ± 0.02	1.00 ± 0.12	0.97 ± 0.11
4N	1.01 ± 0.01	1.18 ± 0.06	0.92 ± 0.06	0.94 ± 0.10
8N	1.23 ± 0.02	1.04 ± 0.03	1.05 ± 0.10	0.94 ± 0.09

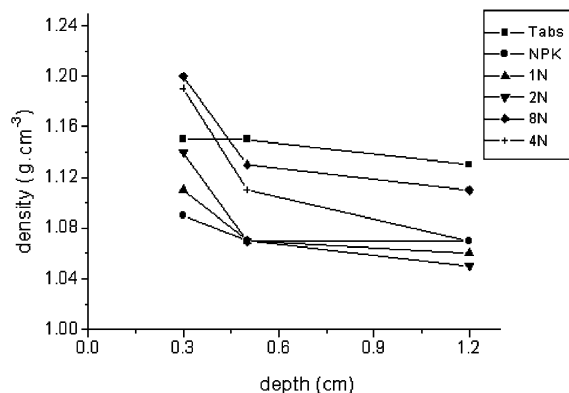


Fig. 10. Gamma-ray transmission analysis of soil density for three depths (3, 5, and 12 mm) for samples of different treatments (Tabs and NPK are controls, 1N, 2N, 4N, and 8N, increasing rates of sewage sludge).

8N. By the analysis of these density profiles it is possible to observe values of ρ significantly higher in the surface layer as compared to the whole sample ρ_s values (Table 2—columns 4 and 5). The results obtained for ρ_{crust} (Figs. 5, 6, 8 and 9) and ρ_s , confirm the existence of a crust sealing process at the soil surface region.

In order to confirm the data obtained by CT, measurements by gamma-ray transmission were also realized in three depths of the samples (Fig. 10). Analyzing the gamma transmission data it is possible to observe that the soil average density decreases with depth, except for the absolute and NPK control treatments. These results confirm the presence of a region with possible sealing of the soil surface layer.

Finally, through of the tomographic image analysis it was possible to estimate the sealing crust thickness that varied from 2 to 4 mm.

5. Conclusion

The gamma-ray CT is a tool that allows a detailed analysis of soil bulk density profiles and the detection of very thin compacted or sealed layers.

Using CT it was possible to confirm the occurrence of soil surface sealing due to the sewage sludge application and it was possible to determine average densities and thickness of these layers.

Acknowledgements

Authors acknowledge FAPESP (grants nos. 00/09048-6 and 00/05732-0) for the financial support.

References

- Baver, L.D., Gardner, W.J., Gardner, W.R., 1973. Física de suelos. Union Tipográfica Editorial Hispano Americana, Mexico, 529pp.
- Bernardes, L.F., 1982. Efeitos da aplicação do lodo de esgoto nas propriedades físicas do solo. Dissertação de mestrado, UNESP/FCAV, Jaboticabal, 50pp.
- Braz, D., Motta, L.M.G., Lopes, R.T., 1999. Computed tomography in the fatigue test analysis of an asphaltic mixture. Appl. Radiat. Isot. 50, 661–671.
- Cássaro, F.A.M., 1994. Tomografia de dupla energia simultânea para caracterização física de um meio poroso deformável. Dissertação de mestrado, EESC/USP, São Carlos, 119pp.
- Crestana, S., Vaz, C.M.P., 1998. Non-invasive instrumentation opportunities for characterizing soil porous systems. Soil Tillage Res. 47, 19–26.
- Crestana, S., Mascarenhas, S., Pozzi-mucelli, R.S., 1985. Static and dynamic three-dimensional studies of water in soil using computerized tomography scanning. Soil Sci. 140, 326–331.
- Epstein, E., 1975. Effects of sewage sludge on some soil physical properties. J. Environ. Qual. 4, 139–142.
- Fante Jr., L., Oliveira, J.C.M., Bassoi, L.H., Vaz, C.M.P., Macedo, A., Bacchi, O.O.S., Reichardt, K., 2000. Evaluation of a soil compaction as concerned to land use. In: Paulo, E.C., Luiz, A.C. (Eds.), Agricultural Tomography. Embrapa—CNPDIA, São Carlos, pp. 125–130.

- Ferraz, E.S.B., Mansell, R.S., 1979. Determining water content and bulk density of soil by gamma-ray attenuation methods. Technical Bulletin, No. 807. IFAS, Flórida, 51pp.
- Hainsworth, J.M., Aylmore, L.A.G., 1983. The use of computer-assisted tomography to determine spatial distribution of soil water content. *Aust. J. Soil Res.* 21, 435–440.
- Logan, T.J., Harrison, B.J., 1995. Physical characteristics of alkaline stabilized sewage sludge (N-Virosol) and their effects on soil physical properties. *J. Environ. Qual.* 24, 153–164.
- Logan, T.J., Harrison, B.J., McAvoy, D.C., Greff, J.A., 1996. Effects of olestra in sewage sludge on soil physical properties. *J. Environ. Qual.* 25, 153–161.
- Lopes, R.T., Bessa, A.P., Braz, D., de Jesus, E.F.O., 1999. Neutron computerized tomography in compacted soil. *Appl. Radiat. Isot.* 50, 451–458.
- Macedo, A., Crestana, S., Vaz, C.M.P., 1998. X-ray microtomography to investigate thin layers of soil clod. *Soil Tillage Res.* 49, 249–253.
- Macedo, A., Vaz, C.M.P., Naime, J.M., Jorge, L.A.C., Crestana, S., Cruvinel, P.E., Pereira, J.C.D., Guimarães, M.F., Ralisch, R., 2000. Soil management impact and wood science—recent contributions of Embrapa Agricultural Instrumentation Center using CT imaging. In: Paulo, E.C., Luiz, A.C. (Eds.), *Agricultural Tomography*. Embrapa—CNPEDIA, São Carlos, pp. 44–54.
- Macedo, J.R., Pires, L.F., Reichardt, K., De Souza, M.D., Bacchi, O.O.S., Meneguelli, N.A., 2001. Utilização de biossólido (lodo de esgoto) e sua influência nas propriedades físicas do solo. In: Delgado, R.V. (Ed.), *CONGRESO LATINOAMERICANO DE LA CIENCIA DEL SUELO*, 15. Resúmenes expandidos, SLCS, Havana, Cuba, CD-ROM.
- Marciano, C.R., 1999. Incorporação de resíduos urbanos e as propriedades físico-hídricas de um Latossolo Vermelho Amarelo. Tese de doutorado, ESALQ/USP, Piracicaba, 93pp.
- Moraes, S.P., 1990. Utilização do composto de lixo em solo agrícola. Dissertação de mestrado, Faculdade de Agronomia/UFRGS, Porto Alegre, 104pp.
- Naime, J.M., 2001. Um novo método para estudos dinâmicos, in situ, da infiltração da água na região não-saturada do solo. Tese de doutorado, EESC/USP, São Carlos, 146pp.
- Naime, J.M., Cruvinel, P.E., Silva, A.M., Crestana, S., Vaz, C.M.P., 2000. Applications of X and γ -rays dedicated computerized tomography scanner in agriculture. In: Paulo, E.C., Luiz, A.C. (Eds.), *Agricultural Tomography*. Embrapa—CNPEDIA, São Carlos, pp. 96–104.
- Pagliai, M., Vignozzi, N., 1998. Use of manure for soil improvement. In: Wallace, A., Terry, R.E. (Eds.), *Handbook of Soil Conditions. Substances that enhance the physical properties of soil*. Marcel Dekker, Inc., New York.
- Petrovic, A.M., Siebert, J.E., Rieke, P.E., 1982. Soil bulk density analysis in three dimensions by computed tomographic scanning. *Soil Sci. Soc. Am. J.* 46, 445–450.
- Pla, I., 1985. A routine laboratory index to predict the effects of soil sealing on soil and water conservation. In: *International Symposium on the assessment of soil surface sealing and crusting*. Ghent, Belgium. ISSS. AISS. IBG, pp. 154–162.
- Robert-Coutant, C., Moulin, V., Sauze, R., Rizo, P., Casagrande, J.M., 1999. Estimation of the matrix attenuation in heterogeneous radioactive waste drums using dual-energy computed tomography. *Nucl. Inst. Phys. Res.* 422, 949–956.
- Wang, C.H., Willis, D.L., Loveland, W.D., 1975. Characteristics of ionizing radiation. In: Wang, C.H., Willis, D.L., Loveland, W.D. (Eds.), *Radiotracer Methodology in the Biological Environmental, and Physical Sciences*. Prentice-Hall, Englewood Cliffs, NJ, pp. 39–74.